Efficient Nuclear DNA Cleavage in Human Cancer Cells by Synthetic Bleomycin Mimics

Li, Qian; van der Wijst, Monique G. P.; Kazemier, Hinke G.; Rots, Marianne G.; Roelfes, Gerard

Published in:
ACS chemical biology

DOI:
10.1021/cb500057n

ACS chemical biology

Articles

pubs.acs.org/acschemicalbiology

Efficient Nuclear DNA Cleavage in Human Cancer Cells by Synthetic Bleomycin Mimics

Qian Li,[†,§] Monique G.P. van der Wijst,[‡,§] Hinke G. Kazemier,[‡] Marianne G. Rots,*[,‡] and Gerard Roelfes*[,†]

[†]Stratingh Institute for Chemistry, University of Groningen, Nijenborgh 4, 9747 AG Groningen, The Netherlands

[‡]Department of Pathology and Medical Biology, University Medical Center Groningen, University of Groningen, Hanzeplein 1, 9713 GZ Groningen, The Netherlands

Supporting Information

ABSTRACT: Iron complexes of *N*,*N*-bis(2-pyridylmethyl)-*N*-bis(2-pyridyl)-methylamine (N4Py) have proven to be excellent synthetic mimics of the Bleomycins (BLMs), which are a family of natural antibiotics used clinically in the treatment of certain cancers. However, most investigations of DNA cleavage activity of these and related metal complexes were carried out in cell-free systems using plasmid DNA as substrate. The present study evaluated nuclear DNA cleavage activity and cell cytotoxicity of BLM and its synthetic mimics based on the ligand N4Py. The N4Py-based reagents induced nuclear DNA cleavage in living cells as efficiently as BLM and Fe(II)-BLM. Treatment of 2 cancer cell lines and 1 noncancerous cell line indicated improved cytotoxicity of N4Py when compared to BLM. Moreover, some level of selectivity was observed for N4Py on cancerous versus noncancerous cells. It was demonstrated that N4Py-based reagents and BLM induce cell death via different mechanistic pathways. BLM was shown to induce cell cycle arrest, ultimately resulting in mitotic catastrophe. In contrast, N4Py-based reagents were shown to induce apoptosis effectively. To the best of our knowledge, the present study is the first demonstration of efficient nuclear DNA cleavage activity of a synthetic BLM mimic within cells. The results presented here show that it is possible to design synthetic bioinorganic model complexes that are at least as active as the parent natural product and thereby are potentially interesting alternatives for BLM to induce antitumor activity.

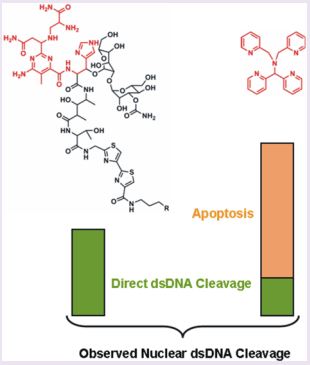

Bleomycins (BLMs) are a family of natural antibiotics produced by *Streptomyces verticillus* first reported in the 1960s.[1] Nowadays, they are widely used for the clinical treatment of various tumors, including carcinoma of cervix, head, neck, and testicles.[2−5] In the presence of cellular metal ions and oxygen, BLMs are capable of mediating oxidative DNA cleavage, which is believed to be the major contributor of their antitumor activity.[3−6] The metal-binding region of BLMs (Figure 1) coordinates metal ions to form metallobleomycins that react with oxygen and consequently mediate the abstraction of H atoms from the DNA substrate to initiate the cascade of DNA cleavage.[4−9] BLM mediates both single (SSBs) and double strand DNA breaks (DSBs) in cells, with the latter proposed to be the main contributor to the observed cytotoxic effects. Depending on the number of DSBs and the ratio of SSB/DSB, two different types of cell death can be induced by BLM.[6,10] Moderate numbers of DSBs lead to cell cycle arrest and mitotic catastrophe, whereas a high number of DSBs, that is, high concentrations of BLM, results in an apoptosis-like process. Experiments with deglycoBLM have shown that a high number of SSBs, or a high SSB/DSB ratio, could act as a signal for the cell to trigger apoptosis.[10]

To date, BLM is among the best studied DNA cleaving antibiotics, although it is still not fully understood in terms of function and mechanism.[7−9,11,12] To better understand BLM's mode of action, different synthetic mimics of the metal-binding domain of BLMs have been designed and synthesized and the study of the corresponding metal complexes has contributed significantly to our understanding.[13−22] Among the metallobleomycins, the highest DNA cleavage activity in cell-free systems is found for Fe-BLM.[4,5,23] With the same level of antitumor activity, the *in vivo* toxicity of Fe(BLM) is significantly less than Cu(BLM) and Zn(BLM) and native BLM at therapeutically effective concentrations.[24] Therefore, intensive studies have been focused on synthetic mimics of Fe-BLM.[15−17,19−22] Many of these mimics are capable of cleaving isolated plasmid DNA, although generally less efficient than Fe-BLM.[15−17,19−22] The cell cytotoxicity of several of these synthetic mimics has been investigated,[20] but to the best of our knowledge, to date there have been no reports demonstrating the actual ability of any of these BLM mimics to induce efficiently nuclear DNA damage in cells.

We previously showed the iron(II) complex of the pentadentate ligand *N*,*N*-bis(2-pyridylmethyl)-*N*-bis(2-pyridyl)-methylamine (N4Py, **1**; Figure 1) to be an excellent structural and functional mimic of Fe(II)-BLM;[22,25−31] efficient cleavage of plasmid DNA was shown for N4Py mimics in cell-free systems, albeit still with lower efficiency than BLM

Received: September 26, 2013
Accepted: February 14, 2014
Published: February 14, 2014

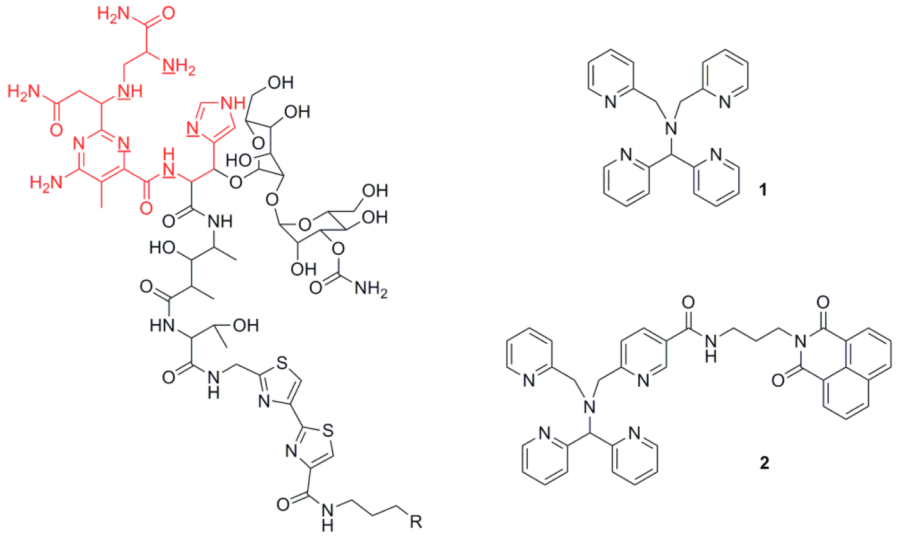

Figure 1. BLM (metal binding domain in red color with metal coordinating N atoms underlined) and N4Py ligands **1** and **2** employed in the present study. Ligand **2** contains a covalently attached 1,8-naphthalimide moiety that could potentially contribute to DNA binding.

itself.[22,28,31] However, these previous data have been obtained in cell-free systems, and might not fully reflect the activity of Fe–N4Py on living cells. Therefore, this study is exploring the cellular responses upon treatment with N4Py-based reagents. Here, we report that, compared to BLM and Fe(II)-BLM, three N4Py-derived synthetic BLM mimics, Fe(II)-**1**, ligand **2** (which contains a covalently attached 1,8-naphthalimide moiety that could potentially contribute to DNA binding), and Fe(II)-**2**, show high cytotoxicity at low micromolar concentrations against the cell lines investigated, with some level of selectivity toward cancer cells. Moreover, the treatment of human carcinoma cells with the N4Py-based reagents gives rise to cell death and nuclear DNA cleavage at least as efficiently as with BLM and Fe(II)-BLM.

RESULTS AND DISCUSSION

Nuclear DNA Damage. The main mechanism of action of BLM and its mimics is thought to proceed *via* the induction of oxidative DNA cleavage.[4−6] For BLM, it has been shown that oxidative DNA cleavage can result in both SSBs and DSBs.[4−6] The latter are the most deleterious form of DNA damage and this can, if left unrepaired, ultimately result in chromosome breaks and translocations, or even be lethal. To validate that the N4Py-based BLM mimics can also induce nuclear DNA damage in living cells, the amount of DSBs was assessed by fluorescence-activated cell sorting (FACS) analysis of γH2AX. The phosphorylated histone variant H2AX (γH2AX) has been well established to be a highly sensitive and specific marker for double-strand breaks in DNA in nuclear chromatin.[32,33]

In this study, the N4Py-based iron(II) complexes Fe(II)-**1** and Fe(II)-**2**, as well as the free ligand **2**, as a representative member of the N4Py ligand family,[22] were used. Based on the high affinity of N4Py ligands for Fe(II) salts,[26] it was expected that this ligand would quickly bind an Fe(II) ion *in vitro*. For comparison, BLM and its corresponding iron complex, Fe(II)-BLM, were included as well. After 48 h of treatment with the reagents, the number of DSBs was determined in two human cancer cell lines (SKOV-3: epithelial ovarian cancer; MDA-MB-231: metastatic breast epithelial cancer) and a noncancerous cell line (HK2: immortalized proximal tubule epithelial cell line from healthy adult human kidney). As the latter are noncancerous yet dividing cells, they provide some indication about the cancer cell line selectivity of the observed effects. The concentration of BLM and BLM mimics used in this study is in the range of reported concentrations of BLM in biological tests *in vitro*.[24,34−37] The HK2 cells were only treated with 30 μM of DNA cleaving agents, except for Fe(II)-BLM, which was also tested at 3 μM.

SKOV-3 and MDA-MB-231 cells treated with 3 μM Fe(II)-**1**, ligand **2**, and Fe(II)-**2** showed similar levels of γH2AX fluorescence as untreated cells or cells treated with solvent only (Figure 2, Supporting Information (SI) Figures S1 and S2, Table S1), so no significant genomic dsDNA damage occurred under these conditions. However, using 3 μM Fe(II)-BLM, γH2AX levels in SKOV-3 cells were 4.2 ± 1.7 fold higher than the solvent controls ($P < 0.05$), which indicates that at this concentration nuclear DNA damage is induced by Fe(II)-BLM.

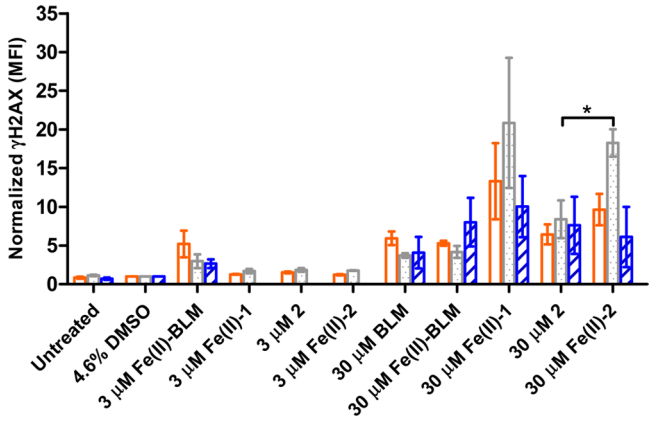

Figure 2. dsDNA damage (γH2AX) upon treatment with BLMs and synthetic BLM mimics. γH2AX mean fluorescence intensity was normalized to solvent control in SKOV-3 (orange), MDA-MB-231 (gray), and HK-2 cells (blue) treated with 3 μM and 30 μM reagents after 48 h. HK-2 cells were only treated with 30 μM reagents, except for 3 μM Fe(II)-BLM. Experiments were conducted by doing each treatment in duplo, and each experiment was carried out in triplicate. Data are presented as the mean ± SEM * $P < 0.05$ compared to all other conditions, according to one-way ANOVA.

dx.doi.org/10.1021/cb500057n | *ACS Chem. Biol.* 2014, 9, 1044−1051

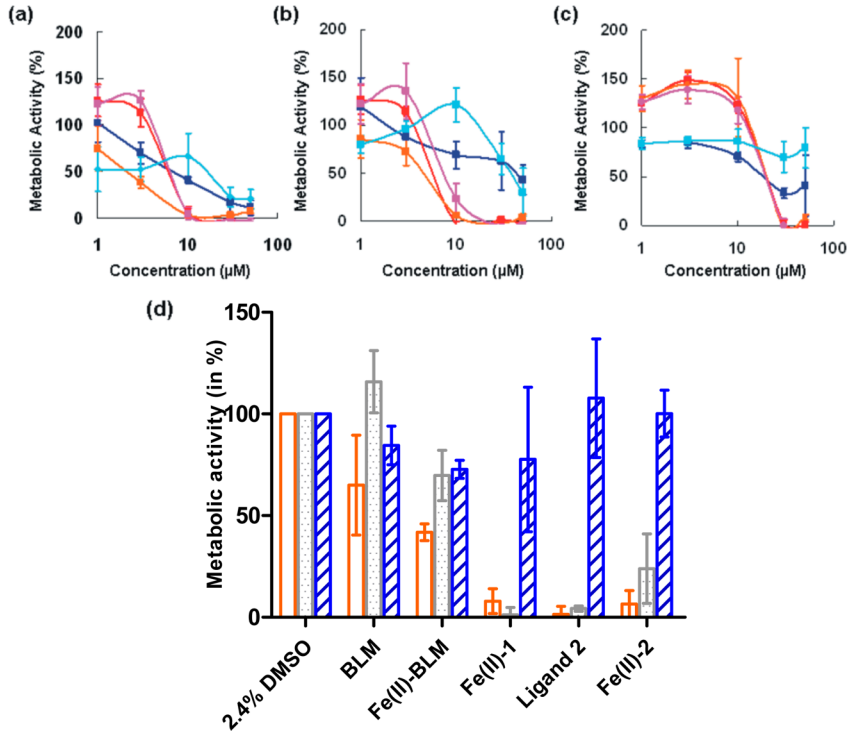

Figure 3. Metabolic activity upon treatment with BLMs and synthetic BLM mimics. Viability of SKOV-3 (a), MDA-MB-231 (b), and noncancerous HK-2 (c) cells treated for 48 h with 1, 3, 10, 30, and 50 μM of BLM (aqua), Fe(II)-BLM (blue), Fe(II)-**1**(red), ligand **2** (orange), and Fe(II)-**2** (pink). Viability of SKOV-3 (orange), MDA-MB-231 (gray), and HK-2 (blue) cells treated with 10 μM of the indicated DNA cleaving agents (d). Experiments were conducted by using triplicate samples for each treatment, and each experiment was carried out in triplicate, or in duplicate in case of BLM. Data are presented as the mean ± SEM.

When the concentration of reagents was increased to 30 μM, the levels of cellular γH2AX fluorescence in both of the cancer cell lines were significantly increased compared to the blank and solvent controls ($P < 0.05$) (Figure 2, SI Figures S3 and S4, Table S1). Thus, efficient nuclear DNA cleavage was induced with all reagents at this concentration (Figure 2, SI Table S2). A comparison between the different N4Py based reagents shows that their activity is comparable (i.e., within the margin of error). The only notable exception is that the observed γH2AX levels in MDA-MB-231 cells induced by 30 μM of the iron complex Fe(II)-**2** are significantly higher than those induced by the uncomplexed ligand **2** at the same concentration ($P < 0.05$). This is in apparent contrast with the observed cytotoxicity for these compounds (*vide infra*).

Metabolic Activity. An MTS (3-(4,5-dimethylthiazol-2-yl)-5-(3-carboxymethoxyphenyl)-2-(4-sulfophenyl)-2H-tetrazolium) assay was performed to determine whether the observed dsDNA damage affected cell functioning.[38,39] The metabolic activity was determined on SKOV-3, MDA-MB-231, and HK2 cells treated for 48 h with different concentrations (1, 3, 10, 30, and 50 μM) of BLM, ligand **2**, and the iron(II) complexes Fe(II)-BLM, Fe(II)-**1**, and Fe(II)-**2**.

As shown in Figure 3a–c, the IC_{50} (half maximal inhibitory concentration) values of BLM and Fe(II)-BLM against SKOV-3 and MDA-MB-231 cancer cells were in the range 10–30 μM, while for the synthetic compounds Fe(II)-**1**, ligand **2**, and Fe(II)-**2** they were in the range 3–10 μM. Against the noncancerous HK-2 cells, the IC_{50} of BLM was >50 μM, while the IC_{50} of Fe(II)-BLM and Fe(II)-**1**, ligand **2**, and Fe(II)-**2** were in the range 10–30 μM. A notable observation is that, whereas the cell viability of SKOV-3 and MDA-MB-231 cancer cells gradually decreased upon increasing the concentration of BLM and Fe-BLM, a sudden transition from good to almost no cell viability was observed in case of the N4Py-based reagents between 3 and 10 μM. The reason for this sudden transition is unclear, but this is in agreement with the observation that at 3 μM concentration of N4Py-based reagents almost no nuclear DNA damage occurred, whereas at 30 μM extensive nuclear DNA damage was observed (Figure 2). Against HK-2 cells, this transition is at higher concentrations, that is, between 10 and 30 μM. Thus, using 10 μM of Fe(II)-**1**, ligand **2**, and Fe(II)-**2**, the viability of SKOV-3 and MDA-MB-231 cancer cells was lost almost completely, while more than 70% of the cell viability of the noncancerous HK-2 cells was remaining (Figure 3d and SI Table S2). Raising the concentration of Fe(II)-**1**, ligand **2** and Fe(II)-**2** to 30 μM, resulted in complete loss of selectivity as also the viability of HK-2 cells was lost completely. With BLM and Fe(II)-BLM, reasonable selectivity in cell viability of the noncancerous HK-2 cells compared to the cancerous SKOV-3 and MDA-MB-231 cells could also be achieved, but only at higher concentrations (i.e., ≥30 μM). Hence, compared to BLM and Fe(II)-BLM, the synthetic mimics showed a higher degree of cancer cell line selective cytotoxicity at low concentration. This is tentatively caused by the higher levels of reactive oxygen species (ROS) in cancer cells compared to normal cells. Cancer cells are known to have elevated levels of ROS including $^1O_2$ and $O_2^{\bullet-}$ compared to normal cells, which is mainly due to the increased metabolism.[40−42] This result is in line with the previously reported plasmid DNA cleavage activity of Fe(II)N4Py complexes, which has been postulated to involve the formation of N4Py-Fe(III)-OOH by reaction with ROS such as $O_2^{\bullet-}$.[22]

Here, the opposite trend is observed for **2** and Fe(II)-**2** compared to the γH2AX assay: in the case of SKOV-3 and

dx.doi.org/10.1021/cb500057n | *ACS Chem. Biol.* 2014, 9, 1044–1051

MDA-MB-231 cells **2** appears to be more cytoxic than Fe(II)-**2** (Figure 3a and b). These observed differences between **2** and its corresponding iron complex are at present not understood. While they suggest that in the cancer cell lines, metal uptake might be a factor, it is not clear how this might relate to the differences observed. A further complicating factor is that multiple processes are involved in cell death caused by N4Py-based reagents (*vide infra*). Since comparable cytotoxicity was observed for Fe(II)-**1** and Fe(II)-**2**, it can be concluded that the covalently attached naphthalimide in ligand **2** does not increase the cytotoxicity.

Apoptotic Effect. Figure 3 shows an improved inhibitory effect on metabolic activity of all N4Py-based reagents compared to the BLMs. However, as the MTS assay only gives a read-out for metabolic activity, the observed decrease herein could be explained by cell growth inhibition (cytostatic) and/or cell death (cytotoxic).

To provide some insight into the mechanism of action, cell death was determined using a propidium iodide (PI)/FACS assay. Cells will only stain PI positive when the cell membrane has become permeable; that is, only late apoptotic or necrotic cells will stain PI positive. For experimental reasons, a comparison was made only between BLM and Fe(II)-**1**, as it is clear from earlier work under cell free conditions and the results above that the naphthalimide moiety in **2** and Fe(II)-**2** does not significantly change the inherent reactivity and the activity *in vitro*. [22]

As high concentrations of DMSO can by itself induce some background level of cell death (SI Figure S5), the DMSO concentration was decreased to 0.1% to reduce background cell death. Remarkably, it was found that 30 μM BLM does not induce significantly more cell death compared to solvent control. In contrast, 30 μM Fe(II)-**1** clearly shows an increase in the percentage of necrotic/late apoptotic cells (77 ± 4.2%) compared to the solvent control (2.6 ± 0.5%) ($P < 0.001$) (Figure 4, SI Table S3, Figure S6).

Different processes may contribute to the observed cell death, including apoptosis, necrosis, and autophagy. It is known that BLM and some of its synthetic mimics are capable of initiating apoptosis.[43,44,20] To address the role of apoptosis with Fe−N4Py, cells were treated with the broad range caspase-inhibitor carbobenzoxy-valyl-alanyl-aspartyl-[O-methyl]-fluoro-methyl-ketone (zVAD-FMK), which is an irreversible inhibitor of the catalytic site of caspase proteases and thereby inhibits apoptosis.[45,46] Upon addition of the apoptosis-inhibitor zVAD-FMK, a relative reduction of 48 ± 9% of cell death in 30 μM Fe(II)-**1** treated cells was found. Hence, about half of the observed cell death under the 30 μM Fe(II)-**1** treatment condition is the result of apoptosis (Figure 4). Even after inhibition of apoptosis, there is still a significant amount of cell death left compared to the solvent control ($P < 0.001$).

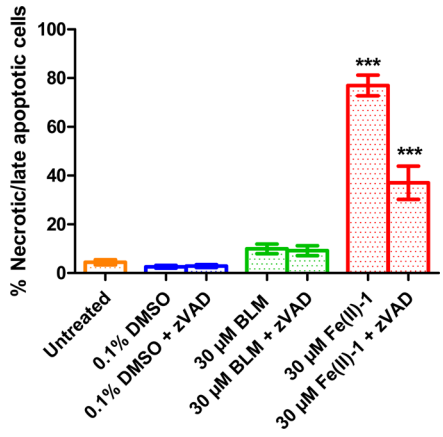

Figure 4. Cell death observed upon treatment with 30 μM BLM and Fe(II)-**1**. SKOV-3 cells were treated for 48 h with 30 μM BLM or Fe(II)-**1** in the presence or absence of the apoptosis-inhibitor zVAD-FMK (20 μM). Flow cytometric analysis of propidium iodide as a cell permeability staining was used to define the percentage of necrotic/late apoptotic cells. Each value represents mean ± SEM from three independent experiments. *** $P < 0.001$ compared to all other conditions, according to one-way ANOVA.

The combined data of Figures 3 and 4 indicate a difference in the mechanism of action of BLM and Fe(II)-**1**; the observed decrease in metabolic activity as seen in Figure 3 is mainly caused by a cytostatic effect of BLM and a cytotoxic effect of Fe(II)-**1**. Thus, in addition to direct N4Py-induced DNA damage, the overall observed nuclear DNA damage (Figure 2) is partially caused indirectly by the induction of apoptosis (Figure 4).[45,47,48]

The contribution of apoptosis in dsDNA cleavage was addressed in our experimental setup by combining flow cytometric analysis of γH2AX with PI. Here, PI was used in a different staining protocol in which it can be used to assess the cell cycle distribution by measuring DNA content.[49,50] All cells containing less DNA than cells in the G1 phase of the cell cycle (the SubG1 peak) resemble (late) apoptotic cells and were excluded from analysis (SI Figure S7, Table S4). By doing so, a better estimation of the direct DNA damage of both reagents could be determined.

A significant amount of γH2AX positive cells within the non/early apoptotic population arose upon treatment of SKOV-3 cells for 48 h with either 30 μM BLM (79 ± 9.0%) or 30 μM Fe(II)-**1** (55 ± 2.5%) versus the solvent control (0.92 ± 0.27%). However, no significant difference in dsDNA damage between both 30 μM DNA cleaving treatments was observed (Figure 5). Interestingly, for 30 μM BLM treated cells, no change in the percentage of γH2AX positive cells was seen when cells were cotreated with zVAD-FMK, which is in line with the minimal cell death observed in BLM treated cells (Figure 4). However, for 30 μM Fe(II)-**1**, it is shown that the amount of γH2AX positive cells was reduced by 51 ± 7.1% after adding zVAD-FMK to the cells ($P < 0.05$). This reduction of γH2AX positive cells equals the reduction in apoptosis as seen in Figure 4. From this, we can conclude that about half of the observed dsDNA damage in the cells still-viable after treatment with 30 μM Fe(II)-**1** is directly induced by apoptosis; the remaining is primarily the result of direct N4Py-induced dsDNA damage.

The above data show that after 48 h of treatment more toxic effects occur for Fe(II)-**1** compared to BLM treatment (Figure 4). Yet, lower levels of directly induced dsDNA damage were seen in Fe(II)-**1** (28 ± 3.9%) versus BLM (74 ± 14%) treated cells ($P < 0.001$) (Figure 5). On the one hand, this reflects the fact that Fe(II)-**1** is a typical single strand DNA cleaving agent, which causes DSBs only after extended single strand cleavage, as has been demonstrated before in cell free conditions using plasmid DNA,[22] whereas BLM is capable of direct double strand DNA cleavage.[4−6,22] Importantly, this also suggests that different mechanisms play a role in the toxicity and generation of DSBs by Fe(II)-**1** versus BLM. Most likely, Fe(II)-**1** is more efficient in inducing (sustained) low level of ssDNA damage.

dx.doi.org/10.1021/cb500057n | *ACS Chem. Biol.* 2014, 9, 1044−1051

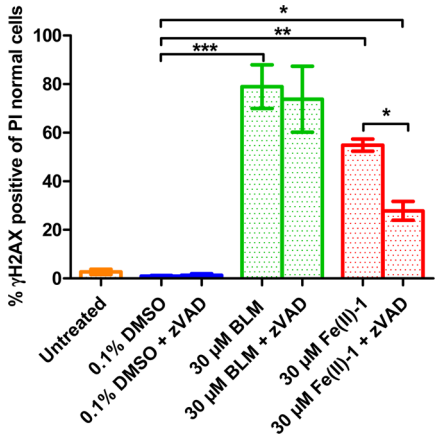

Figure 5. dsDNA damage (γH2AX) in non/early apoptotic cells. SKOV-3 cells were treated for 48 h with 30 μM BLM or Fe(II)-**1** in the presence or absence of the apoptosis-inhibitor zVAD-FMK (20 μM). Flow cytometric analysis of γH2AX, a marker for dsDNA damage, was used in combination with propidium iodide, a marker for DNA content, to exclude late apoptotic cells (in the subG1 peak) from analysis. The γH2AX positive population was defined based on about 1% positivity in the 0.1% DMSO treated cells. Each value represents mean ± SEM from at least three independent experiments. * $P < 0.05$; ** $P < 0.01$; *** $P < 0.001$ compared to all other conditions, according to one-way ANOVA.

When enough SSBs accumulate, these could act as signals to induce apoptosis, analogous to the reported activity of deglycoBLM.[10] As a consequence of the apoptosis process, then, DSBs occur. In contrast, at low numbers of DSBs the cytoxity of BLM is caused by cell cycle arrest followed by mitotic catastrophe.[10] Another explanation for the higher toxicity of Fe(II)-**1** versus BLM might be that Fe(II)-**1** not only damages molecules within the nucleus but also in other compartments of the cell, which then also results in triggering of apoptosis.

The proposed difference in mechanism of cell death is further illustrated by comparing BLM and Fe(II)-**1** in a clonogenic assay.[51] After a 1 h or 8 h treatment with either 30 μM BLM, 30 μM Fe(II)-1, or 0.1% DMSO, SKOV3 cells were reseeded in fresh media at a density of 750 cells/6 well. After 20 days, the colony forming potential was assessed by counting the number of colonies formed (≥50 cells/colony). During treatment, neither BLM or Fe(II)-**1** induced significant cell death. Figure 6a shows that BLM is already very potent in inhibiting the colony forming potential after only 1 h treatment. In contrast, the inhibitory effects of Fe(II)-**1** on the colony forming potential become visible only after an 8 h treatment (Figure 6b). This clearly indicates that the mechanism in which both reagents damage the cell is different. Combined with the FACS data (Figures 4 and 5, SI Figure S8), these results confirm that 30 μM BLM mainly affects the cell via the induction of a G2/M-phase cell cycle arrest through the induction of DSBs (Figure 5). As a consequence, either a lack of proliferation or cell death induced via mitotic catastrophe results in virtually none of the cells capable of forming colonies anymore already after 1 h treatment. On the other hand, Fe(II)-**1** does not affect the cell cycle (SI Figure S8) but induces damage in the cell. Only after 8 h treatment the accumulated damage is such that apoptosis is triggered, resulting in cell death and thus the colony forming potential is significantly reduced compared to 0.1% DMSO treatment.

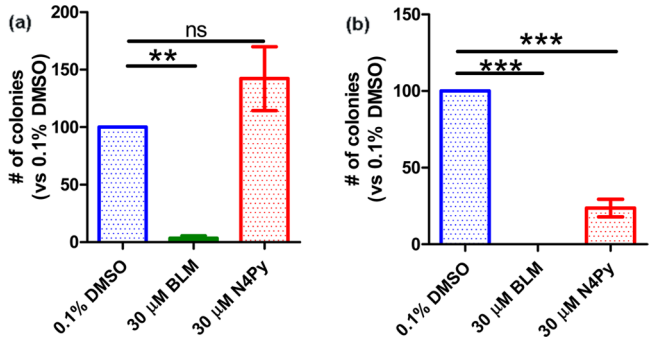

Figure 6. Colony forming potential upon treatment with 30 μM BLM and Fe(II)-**1**. After 1 h (a) or 8 h (b) treatment with either 30 μM BLM, Fe(II)-**1**, or 0.1% DMSO, SKOV-3 cells were reseeded in fresh media (750 cells/6 well). After 20 days, the colony forming potential was determined relative to 0.1% DMSO treatment. Each value represents mean ± SEM from at least three independent experiments. ** $P < 0.01$; *** $P < 0.001$; ns = not significant, compared to all other conditions, according to one-way ANOVA.

CONCLUSION

The results presented here are the first demonstration of the nuclear DNA cleavage activity of a synthetic BLM mimic. It was found that Fe(II)-**1**, ligand **2**, and Fe(II)-**2** were cytotoxic for SKOV-3 and MDA-MB-231 cancer cells at low micromolar concentrations while displaying some degree of cancer cell line selectivity; that is, at the same concentrations, the viability of noncancerous HK-2 cells was not affected significantly. Treatment of SKOV-3 and MDA-MB-231 cancer cells with N4Py-based mimics gave rise to DSBs at least as efficient as with BLM. The DSBs induced by treatment with BLM were the result of a direct effect, that is, BLM induced nuclear dsDNA cleavage, resulting in cell cycle arrest. In contrast, the observed DSBs of Fe(II)-**1** are partially caused by the triggering of apoptosis, tentatively ascribed to a combination of sustained ssDNA cleavage and indirect effects such as oxidative damage of other cellular components. Nevertheless, besides the apoptosis-related DSBs, also significant direct oxidative DNA cleavage by the N4Py-based mimics occurs (summarized in Figure 7).

In conclusion, our results convincingly show that it is possible to design synthetic bioinorganic model complexes that are at least as active as the parent natural product, even if they function through a different mechanism, thus underlining the power of the bioinorganic modeling approach.

METHODS

Materials. All reagents and solvents were used as purchased without further purification unless noted otherwise. Bleomycin sulfate (A_2 + B_2, 95%), from *Streptomyces verticillus*, was purchased from Calbiochem. Ligands **1** and **2** were synthesized according to literature procedures and all characterization data are in agreement with those reported.[22] Iron(II) complex of ligand **1** was obtained as [MeCN·Fe(II)·N_4Py]$(ClO_4)_2$·$2H_2O$ by crystallization, as previously published.[25] $(NH_4)_2Fe^{II}(SO_4)_2$ (1 equiv.) was added to solutions of BLM and ligand **2** in 1:1 DMSO/H_2O to generate the corresponding iron(II) complexes *in situ*. The broad range caspase-inhibitor carbobenzoxy-valyl-alanyl-aspartyl-[O-methyl]-fluoromethyl-ketone (zVAD-FMK) was bought from Calbiochem.

Cell Culture. The human ovarian carcinoma cell line SKOV-3 (HTB-77), the human mammary gland adenocarcinoma cell line MDA-MB-231 (HTB-26), and the immortalized proximal tubule epithelial cell line from normal adult human kidney HK-2 (CRL-2190) were obtained from the ATCC (Manassas, VA). SKOV-3 and MDA-MB-231 were cultured in Dulbecco's modified Eagle's medium

dx.doi.org/10.1021/cb500057n | *ACS Chem. Biol.* 2014, 9, 1044−1051

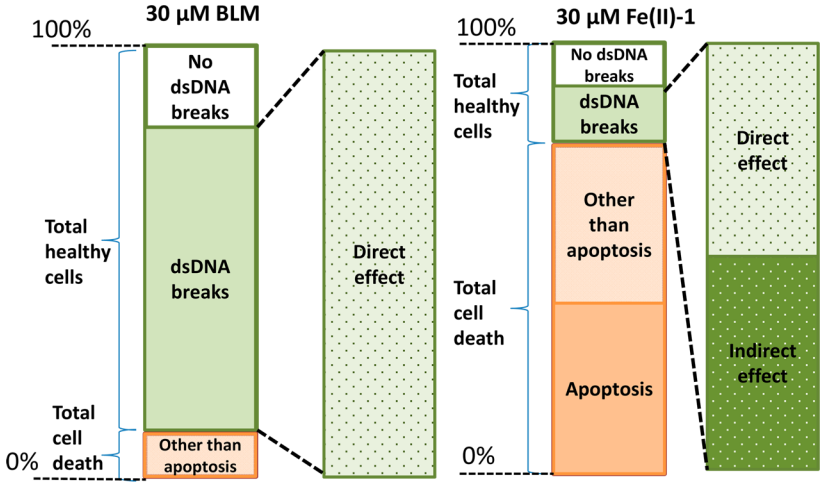

Figure 7. Differential effect on living cells of 30 μM BLM vs 30 μM N4Py treatment. SKOV-3 cells treated for 48 h with either 30 μM BLM or 30 μM N4Py show a different response to each treatment. 30 μM BLM directly induces a large amount of dsDNA breaks compared to 30 μM N4Py. Nevertheless, more cells are dying upon treatment with 30 μM N4Py compared to 30 μM BLM.

(DMEM) (Lonza, Verviers, Belgium) supplemented with 10% FCS (Perbio Hyclone, Etten-Leur, The Netherlands), 50 μg/mL gentamycine sulfate (Invitrogen, Breda, The Netherlands), 2 mM L-glutamine (Lonza). HK-2 was cultured in 1:1 mixture DMEM and Ham's F-12 (Invitrogen) supplemented with 10% FCS, 1% penicillin/streptomycin (Invitrogen), 0.01 mg/L EGF(Tebu-Bio, Heerhugowaard, The Netherlands), 10 mg/L insulin, 5.5 mg/L transferrin, 6.7 ug/L sodium selenite (ITS) (Invitrogen), 36 ug/L hydrocortisone (Sigma-Aldrich Chemie B.V., Zwijndrecht, The Netherlands), 2 mM glutamax (Invitrogen). Cell cultures were incubated at 37 °C under humidified conditions and 5% CO_2.

***In Vitro* Cytotoxicity.** The viability of cells in the presence and absence of reagents was determined by using the MTS assay. SKOV-3 and MDA-MB-231 cells were seeded at a density of $2 \times 10^4/cm^2$ in 96-well plates (Corning Inc., Corning, NY), HK-2 cells were seeded at $1.5 \times 10^4/cm^2$. At 70−80% confluence, the culture medium was replaced by fresh medium containing reagents. All DNA cleaving reagents were dissolved in 1:1 DMSO/H_2O to obtain final concentrations of 0, 1, 3, 10, 30, and 50 μM in 100 μL culture medium. The final concentration of DMSO in culture medium was 2.4% (v/v). Controls were treated with same concentrations (v/v) of 1:1 DMSO/H_2O only. After 48 h, 20 μL of fresh CellTiter 96 Aqueous One Solution (Promega, Madison, WI) was added and incubated for 3 h. The absorbance at 490 nm was measured using a Varioskan plate reader (Thermo Electron Corp., Breda, The Netherlands) and subtracted with the absorbance of cell-free medium containing reagents. Experiments were conducted by using triplicate samples for each treatment and each experiment was carried out at least three times unless noted otherwise.

Cell Death Analysis. SKOV-3 cells were seeded at a density of $2.85 \times 10^4/cm^2$ in 12-well plates (Corning Inc.). The following day, culture medium was replaced with fresh medium containing reagents. All DNA cleaving reagents were dissolved in 1:1 DMSO/H_2O to obtain a final concentration of 3 and 30 μM in the medium. Apoptosis was inhibited by addition of zVAD-FMK (20 μM final concentration) to the medium. The final concentration of DMSO in culture medium was 0.1% (v/v). Controls were treated with same concentrations (v/v) of 1:1 DMSO/H_2O only. 48 h after treatment, both floating and adherent cells were harvested and stained with 5 μg/mL PI (Sigma-Aldrich Chemie B.V.)/PBS. After a 10 min incubation at 4 °C in the dark, fluorescence was measured using the FL-3 channel of a FACScalibur flow cytometer (Beckton Dickenson Biosciences, San Jose, CA). Experiments were conducted in triplicate. Percentages PI positive cells were determined with Kaluza 1.2 (Beckman Coulter) software and graphs were made using Kaluza 1.2 (Beckman Coulter) and Graphpad Prism 5 software (GraphPad Software Inc., La Jolla, CA).

dsDNA Breaks. The ability of the reagents under investigation to induce dsDNA damage was tested using intracellular γH2AX staining with flow cytometry read-out as described in literature.[52] In short, SKOV-3 and MDA-MB-231 cells were seeded at a density of $2.85 \times 10^4/cm^2$ in 12-well plates (Corning Inc.). At 70−80% confluence, the culture medium was replaced with fresh medium containing reagents. All DNA cleaving reagents were dissolved in 1:1 DMSO/H_2O to obtain a final concentration of 3 and 30 μM in the medium. Apoptosis was inhibited by concurrently adding 20 μM zVAD-FMK to the well. The final concentration of DMSO in culture medium was 4.6% (v/v) for Figure 2 and 0.1% for Figure 5. Controls were treated with same concentrations (v/v) of 1:1 DMSO/H_2O only. Both floating and adherent cells treated with different reagents were harvested after 48 h, and fixed in 4% formaldehyde (Merck, Darmstadt, Germany)/PBS for 10 min at 37 °C and permeabilized in 90% methanol/PBS for 30 min on ice. Cells were resuspended in 100 μL PBS containing 50 μg phospho-histone H2A.X (ser139) (20E3) rabbit mAb (Alexa Fluor 488 conjugate) (Cell Signaling, Leiden, The Netherlands), and 0.5% BSA. After a 30 min incubation in the dark at RT, cells were washed with PBS and fluorescence was determined in the FL1 channel of a FACScalibur flow cytometer.

The amount of dsDNA breaks in the healthy/early apoptotic population was determined by adding PI, used as a DNA content marker, to the staining.[49,50] Fixed and permeabilized cells were resuspended in 100 μL PBS containing 50 μg of Phospho-Histone H2A.X (ser139) (20E3) Rabbit mAb (Alexa Fluor 488 conjugate), 10 μg RNase A (Qiagen, Utrecht, The Netherlands), and 0.5% BSA. After a 30 min incubation in the dark at RT, cells were washed in PBS. Cells were resuspended in 5 μg/mL PI/PBS and after a 10 min incubation in the dark at 4 °C, fluorescence was measured in the FL-1 channel for γH2AX-Alexa Fluor 488 and the FL-2 channel for PI using a FACScalibur flow cytometer. Cells in the subG1 population were excluded from analysis of dsDNA breaks in early/non-apoptotic cells. The cutoff for a γH2AX positive cell was set based on a level of ~1% positivity in the solvent control. Experiments were conducted by using duplicate samples for each treatment, and each experiment was carried out at least three times unless noted otherwise. MFI and PI low cells were determined with WinList and Kaluza 1.2 (Beckman Coulter) software. Graphs were made using WinMDI, Kaluza 1.2 (Beckman Coulter) and Graphpad Prism 5 software.

Clonogenic Assay. The inhibitory effects of BLM and Fe(II)-**1** on the colony forming potential were tested as described in literature.[53] After 1 h or 8 h treatment with either 30 μM BLM, 30 μM Fe(II)-**1** or 0.1% DMSO, SKOV-3 cells were reseeded in 6-well plates (750 cells/well) containing fresh media. After 20 days, media was replaced by Coomassie brilliant blue (Bio-Rad). The colony forming potential was

dx.doi.org/10.1021/cb500057n | *ACS Chem. Biol.* 2014, 9, 1044−1051

determined by counting the number of colonies (≥50 cells) using phase-contrast microscopy

Statistics Calculation. All FACS and MTS data are presented as the mean ± SEM. These data were evaluated by one-way ANOVA and considered statistically significant with a p value <0.05.

■ ASSOCIATED CONTENT

Supporting Information

FACS analysis of nuclear DNA damage; cell cytotoxicity; apoptotic effect. Figures S1−S8, Tables S1−S4. This material is available free of charge *via* the Internet at http://pubs.acs.org.

■ AUTHOR INFORMATION

Corresponding Authors

*E-mail: M.G.Rots@umcg.nl.

*E-mail: j.g.roelfes@rug.nl.

Author Contributions

§Q.L. and M.G.P.v.d.W. contributed equally to this work.

Notes

The authors declare no competing financial interest.

■ ACKNOWLEDGMENTS

We gratefully acknowledge J. M. Dokter-Fokkens and S. de Rond for cell cultures and R. van der Lei and G. Mesander for FACS analysis. We also thank the University of Groningen and the University Medical Center Groningen for financial support. This work was supported by The Netherlands Organization for Scientific Research (NWO) through a CHEMTHEM grant, grant No.728.011.101.

■ REFERENCES

(1) Umezawa, H., Maeda, K., Takeuchi, T., and Okami, Y. (1966) New antibiotics, bleomycin A and B. *J. Antibiot. 19*, 200−209.

(2) Blum, R. H., Carter, S. K., and Agre, K. (1973) A clinical review of bleomycin—A new antineoplastic agent. *Cancer 31*, 903−914.

(3) Kross, J., Henner, W. D., Hecht, S. M., and Haseltine, W. A. (1982) Specificity of deoxyribonucleic acid cleavage by bleomycin, phleomycin, and tallysomycin. *Biochemistry 21*, 4310−4318.

(4) Burger, R. M. (1998) Cleavage of nucleic acids by bleomycin. *Chem. Rev. 98*, 1153−1170.

(5) Hecht, S. M. (2000) Bleomycin: New perspectives on the mechanism of action. *J. Nat. Prod. 63*, 158−168.

(6) Chen, J. Y., and Stubbe, J. (2005) Bleomycins: Toward better therapeutics. *Nat. Rev. Cancer 5*, 102−112.

(7) Loeb, K. E., Zaleski, J. M., Hess, C. D., Hecht, S. M., and Solomon, E. I. (1998) Spectroscopic investigation of the metal ligation and reactivity of the ferrous active sites of bleomycin and bleomycin derivatives. *J. Am. Chem. Soc. 120*, 1249−1259.

(8) Neese, F., Zaleski, J. M., Zaleski, K. L., and Solomon, E. I. (2000) Electronic structure of activated bleomycin: Oxygen intermediates in heme versus non-heme iron. *J. Am. Chem. Soc. 122*, 11703−11724.

(9) Decker, A., Chow, M. S., Kemsley, J. N., Lehnert, N., and Solomon, E. I. (2006) Direct hydrogen-atom abstraction by activated bleomycin: An experimental and computational study. *J. Am. Chem. Soc. 128*, 4719−4733.

(10) Tounekti, O., Kenani, A., Foray, N., Orlowski, S., and Mir, L. M. (2001) The ratio of single- to double-strand DNA breaks and their absolute values determine cell death pathway. *Br. J. Cancer 84*, 1272−1279.

(11) Goodwin, D. D., Lewis, M. A., Long, E. C., and Georgiadis, M. M. (2008) Crystal structure of DNA-bound Co(III)·bleomycin B_2: Insights on intercalation and minor groove binding. *Proc. Natl. Acad. Sci. U.S.A. 105*, 5052−5056.

(12) Bozeman, T. C., Nanjunda, R., Tang, C., Liu, Y., Segerman, Z. J., Zaleski, P. A., Wilson, W. D., and Hecht, S. M. (2012) Dynamics of bleomycin interaction with a strongly bound hairpin DNA substrate, and implications for cleavage of the bound DNA. *J. Am. Chem. Soc. 134*, 17842−17845.

(13) Brown, S. J., Stephan, D. W., and Mascharak, P. K. (1988) Characterization of a crystalline synthetic analog of copper(II)-bleomycin. *J. Am. Chem. Soc. 110*, 1996−1997.

(14) Tan, J. D., Hudson, S. E., Brown, S. J., Olmstead, M. M., and Mascharak, P. K. (1992) Syntheses, structures, and reactivities of synthetic analogs of the three forms of cobalt(III)-bleomycin: Proposed mode of light-induced DNA damage by the cobalt(III) chelate of the drug. *J. Am. Chem. Soc. 114*, 3841−3853.

(15) Guajardo, R. K., Hudson, S. E., Brown, S. J., and Mascharak, P. K. (1993) $[Fe(PMA)]^{n+}$ (n = 1,2): Good models of iron-bleomycins and examples of mononuclear non-heme iron complexes with significant oxygen-activation capabilities. *J. Am. Chem. Soc. 115*, 7971−7977.

(16) Lippai, I., Magliozzo, R. S., and Peisach, J. (1999) EPR spectroscopic reinvestigation of the activation of iron complexes of PMAH as a bleomycin model. *J. Am. Chem. Soc. 121*, 780−784.

(17) Mialane, P., Nivorojkine, A., Pratviel, G., Azéma, L., Slany, M., Godde, F., Simaan, A., Banse, F., Kargar-Grisel, T., Bouchoux, G., Sainton, J., Horner, O., Guilhem, J., Tchertanova, L., Meunier, B., and Girerd, J.-J. (1999) Structures of Fe(II) complexes with N,N,N′-tris(2-pyridylmethyl) ethane-1,2-diamine type ligands. Bleomycin-like DNA cleavage and enhancement by an alkylammonium substituent on the N′ atom of the ligand. *Inorg. Chem. 38*, 1085−1092.

(18) Kurosaki, H., Hayashi, K., Ishikawa, Y., Goto, M., Inada, K., Taniguchi, I., Shionoya, M., and Kimura, E. (1999) New robust bleomycin analogues: Synthesis, spectroscopy, and crystal structures of the Copper(II) complexes. *Inorg. Chem. 38*, 2824−2832.

(19) Hemmert, C., Pitié, M., Renz, M., Gornitzka, H., Soulet, S., and Meunier, B. (2001) Preparation, characterization and crystal structures of manganese(II), iron(III) and copper(II) complexes of the bis[di-1,1-(2-pyridyl)ethyl]amine (BDPEA) ligand; evaluation of their DNA cleavage activities. *J. Biol. Inorg. Chem. 6*, 14−22.

(20) Wong, E. L.-M., Fang, G.-S., Che, C.-M., and Zhu, N. (2005) Highly cytotoxic iron(II) complexes with pentadentate pyridyl ligands as a new class of anti-tumor agents. *Chem. Commun.*, 4578−4580.

(21) Mukherjee, A., Dhar, S., Nethaji, M., and Chakravarty, A. R. (2005) Ternary iron(II) complex with an emissive imidazopyridine arm from Schiff base cyclizations and its oxidative DNA cleavage activity. *Dalton Trans.*, 349−353.

(22) Li, Q., van den Berg, T. A., Feringa, B. L., and Roelfes, G. (2010) Mononuclear Fe(II)-N4Py complexes in oxidative DNA cleavage: Structure, activity, and mechanism. *Dalton Trans.*, 8012−8021.

(23) Sausville, E. A., Peisach, J., and Horwitz, S. B. (1978) Effect of chelating agents and metal ions on the degradation of DNA by bleomycin. *Biochemistry 17*, 2740−2746.

(24) Rao, E. A., Saryan, L. A., Antholine, W. E., and Petering, D. H. (1980) Cytotoxic and antitumor properties of bleomycin and several of its metal complexes. *J. Med. Chem. 23*, 1310−1318.

(25) Lubben, M., Meetsma, A., Wilkinson, E. C., Feringa, B. L., and Que, L., Jr. (1995) Nonheme iron centers in oxygen activation: characterization of an iron(III) hydroperoxide intermediate. *Angew. Chem., Int. Ed. Engl. 34*, 1512−1514.

(26) Roelfes, G., Lubben, M., Chen, K., Ho, R. Y. N., Meetsma, A., Genseberger, S., Hermant, R. M., Hage, R., Mandal, S. K., Young, V. G., Jr., Zang, Y., Kooijman, H., Spek, A. L., Que, L., Jr., and Feringa, B. L. (1999) Iron chemistry of a pentadentate ligand that generates a metastable Fe^{III}−OOH intermediate. *Inorg. Chem. 38*, 1929−1936.

(27) Ho, R. Y. N., Que, L., Jr., Roelfes, G., Feringa, B. L., Hermant, R., and Hage, R. (1999) Resonance Raman evidence for the interconversion between an $[Fe^{III}-\eta^1\text{-}OOH]^{2+}$ and $[Fe^{III}-\eta^2\text{-}O_2]^+$ species and mechanistic implications thereof. *Chem. Commun.*, 2161−2162.

(28) Roelfes, G., Branum, M. E., Wang, L., Que, L., Jr., and Feringa, B. L. (2000) Efficient DNA cleavage with an iron complex without added reductant. *J. Am. Chem. Soc. 122*, 11517−11518.

(29) Lehnert, N., Neese, F., Ho, R. Y. N., Que, L., Jr., and Solomon, E. I. (2002) Electronic structure and reactivity of low-spin Fe(III)−hydroperoxo complexes: Comparison to activated bleomycin. *J. Am. Chem. Soc. 124*, 10810−10822.
(30) Roelfes, G., Vrajmasu, V., Chen, K., Ho, R. Y. N., Rohde, J., Zondervan, C., la Crois, R. M., Schudde, E. P., Lutz, M., Spek, A. L., Hage, R., Feringa, B. L., Münck, E., and Que, L., Jr. (2003) End-on and side-on peroxo derivatives of non-heme iron complexes with pentadentate ligands: Models for putative intermediates in biological iron/dioxygen chemistry. *Inorg. Chem. 42*, 2639−2653.
(31) van den Berg, T. A., Feringa, B. L., and Roelfes, G. (2007) Double strand DNA cleavage with a binuclear iron complex. *Chem. Commun.*, 180−182.
(32) Olive, P. L. (2004) Detection of DNA damage in individual cells by analysis of histone H2AX phosphorylation. *Methods Cell Biol. 75*, 355−373.
(33) Bonner, W. M., Redon, C. E., Dickey, J. S., Nakamura, A. J., Sedelnikova, O. A., Solier, S., and Pommier, T. (2008) γH2AX and cancer. *Nat. Rev. Cancer 8*, 957−967.
(34) Barranco, S. C., and Humphrey, R. M. (1971) The effects of bleomycin on survival and cell progression in Chinese hamster cells *in vitro*. *Cancer Res. 31*, 1218−1223.
(35) Lin, P. S., Kwock, L., Hefter, K., and Misslbeck, G. (1983) Effects of iron, copper, cobalt, and their chelators on the cytotoxicity of bleomycin. *Cancer Res. 43*, 1049−1053.
(36) Byrnes, R. W., Templin, J., Sem, D., Lyman, S., and Petering, D. H. (1990) Intracellular DNA strand scission and growth inhibition of *Ehrlich ascites* tumor cells by bleomycins. *Cancer Res. 50*, 5275−528.
(37) Pron, G., Mahrour, N., Stéphane Orlowski, S., Tounekti, O., Poddevin, B., Belehradek, J., and Mir, L. M. (1999) Internalisation of the bleomycin molecules responsible for bleomycin toxicity: A receptor-mediated endocytosis mechanism. *Biochem. Pharmacol. 57*, 45−56.
(38) Scudiero, D. A., Shoemaker, R. H., Paull, K. D., Monks, A., Tierney, S., Nofziger, T. H., Currens, M. J., Seniff, D., and Boyd, M. R. (1988) Evaluation of a soluble tetrazolium/formazan assay for cell growth and drug sensitivity in culture using human and other tumor cell lines. *Cancer Res. 48*, 4827−4833.
(39) Cory, A. H., Owen, T. C., Barltrop, J. A., and Cory, J. G. (1991) Use of an aqueous soluble tetrazolium/formazan assay for cell growth assays in culture. *Cancer Commun. 3*, 207−212.
(40) Toyokuni, S., Okamoto, K., Yodoi, J., and Hiai, H. (1995) Persistent oxidative stress in cancer. *FEBS Lett. 358*, 1−3.
(41) Gupte, A., and Mumper, R. J. (2009) Elevated copper and oxidative stress in cancer cells as a target for cancer treatment. *Cancer Treat. Rev. 35*, 32−46.
(42) Trachootham, D., Alexandre, J., and Huang, P. (2009) Targeting cancer cells by ROS-mediated mechanisms: A radical therapeutic approach? *Nat. Rev. Drug Discovery 8*, 579−591.
(43) Vernole, P., Tedeschi, B., Caporossi, D., Maccarrone, M., Melino, G., and Annicchiarico-Petruzzelli, M. (1998) Induction of apoptosis by bleomycin in resting and cycling human lymphocytes. *Mutagenesis 13*, 209−215.
(44) Mungunsukh, O., Griffin, A. J., Lee, Y. H., and Regina M. Day, R. M. (2010) Bleomycin induces the extrinsic apoptotic pathway in pulmonary endothelial cells. *Am. J. Physiol. Lung Cell Mol. Physiol. 298*, 696−703.
(45) Samejima, K., and Earnshaw, W. C. (2005) Trashing the genome: The role of nucleases during apoptosis. *Nat. Rev. Mol. Cell Biol. 6*, 677−688.
(46) Callus, B. A., and Vaux, D. L. (2007) Caspase inhibitors: Viral, cellular, and chemical. *Cell Death Differ. 14*, 73−78.
(47) Compton, M. M. (1992) A biochemical hallmark of apoptosis: Internucleosomal degradation of the genome. *Cancer Metast. Rev. 11*, 105−119.
(48) Riedl, S. J., and Shi, Y. (2004) Molecular mechanisms of caspase regulation during apoptosis. *Nat. Rev. Mol. Cell Biol. 5*, 897−907.
(49) Darzynkiewicz, Z., Juan, G., Li, X., Gorczyca, W., Murakami, T., and Traganos, F. (1997) Cytometry in cell necrobiology: Analysis of apoptosis and accidental cell death (necrosis). *Cytometry 27*, 1−20.
(50) Wlodkowic, D., Skommer, J., and Darzynkiewicz, Z. (2009) Flow cytometry-based apoptosis detection. *Methods Mol. Biol. 559*, 19−32.
(51) Franken, N. A., Rodermond, H. M., Stap, J., Haveman, J., and van Bree, C. (2006) Clonogenic assay of cells *in vitro*. *Nat Protoc. 1*, 2315−2319.
(52) Geel, T. M., Meiss, G., van der Gun, B. T., Kroesen, B. J., de Leij, L. F., Zaremba, M., Šilanskas, A., Kokkinidis, M., Pingoud, A., Ruiters, M. H., McLaughlin, P. M., and Rots, M. G. (2009) Endonucleases induced TRAIL-insensitive apoptosis in ovarian carcinoma cells. *Exp. Cell Res. 315*, 2487−2495.
(53) Huisman, C., Wisman, G. B., Kazemier, H. G., van Vugt, M. A., van der Zee, A. G., Schuuring, E., and Rots, M. G. (2013) Functional validation of putative tumor suppressor gene C13ORF18 in cervical cancer by artificial transcription factors. *Mol Oncol. 7*, 669−679.